Particle Production by 2.9-BeV Protons Incident on Beryllium and Platinum*

P. A. Piroué and A. J. S. Smith
Palmer Physical Laboratory, Princeton University, Princeton, New Jersey
(Received 31 March 1966)

Differential cross sections as a function of momentum are presented for the production of π mesons, K mesons, protons, deuterons, tritons, and He^3 at various laboratory angles by 2.9-BeV protons striking Be and Pt targets. The Be data were taken at 13°, 30°, 60°, and 93° relative to the direction of the Princeton-Pennsylvania Accelerator internal proton beam; the Pt data were taken at 13° and 93° only. The results are compared with the corresponding data in hydrogen in order to investigate the role of the complex nucleus in particle production at this energy.

I. INTRODUCTION AND SUMMARY

THE present work is a contribution to the beam survey program which was carried out at the Princeton-Pennsylvania Accelerator (PPA) in the summer of 1963 when the synchrotron started to operate. Additional data were taken later whenever possible. Preliminary results from other contributors[1–3] have already been reported.

The main objective of the program was the determination, as a function of momentum, of differential cross sections at various laboratory angles for the production of a variety of particles by 2.9-BeV protons striking beryllium and platinum targets. Such data are particularly useful in the planning of experiments and the design of secondary beams. Although similar work has been done at much higher energies[4–11] there has been very little information on particle production in complex nuclei at 3 BeV.[12]

The beryllium data were taken at 13°, 30°, 60°, and 93° relative to the direction of the PPA internal proton beam; the platinum data were taken at 13° and 93° only. Among the particles studied are $\pi^{\pm}$ mesons, K^+ mesons, protons, deuterons, tritons, and He^3; K^- mesons were observed at 13°. In a separate experiment performed in collaboration with a Columbia University group, production of antiprotons was observed in copper at 13° for incident proton energies of 2.88 and 3.05 BeV; these results have already been reported.[13]

For each particle the results are compared to the corresponding data in hydrogen in order to investigate the role of the complex nucleus in particle production at this energy.

It is found that the pion and kaon data can be explained in terms of collisions of incident protons with individual target nucleons. Fermi motion has little effect. On the other hand, the production of deuterons, tritons, and He^3 *cannot* be so explained; the presence of nuclear matter is necessary to account for the experimental observations. The deuteron results are analyzed in terms of a model[6,14] which has been reasonably successful in interpreting the general features of deuteron production in complex nuclei at higher energies. Proton production, as one might expect, results both from nucleon-nucleon encounters and processes involving nuclear matter. Finally, previous antiproton results used to investigate high momentum components of Fermi motion are reviewed.

II. EXPERIMENTAL ARRANGEMENT

A. Beams and Detectors

Figure 1 shows the layout of the beams used during the survey period. The internal target, 1 in. long, $\frac{1}{2}$ in. wide, and $\frac{1}{4}$ in. high, could be viewed through six channels located at 13°, 30°, 45°, 60°, 75°, and 93° relative to the direction of the PPA internal proton beam. Except for the 45° and 75° channels, which were used to monitor the beam on target, each secondary beam channel consisted of a quadrupole doublet,

* This work was supported by the U. S. Office of Naval Research, Contract No. Nonr-1858(06).

[1] T. J. Devlin, PPAD 502 C, Princeton-Pennsylvania Accelerator, Princeton University, Princeton, New Jersey, 1963 (unpublished).

[2] E. Miller and G. L. Salmon, PPAD 505 C, Princeton-Pennsylvania Accelerator, Princeton University, Princeton, New Jersey, 1963 (unpublished).

[3] A. Berick, D. Hansen, C. Ward, and C. York, Physics Department Report, University of California at Los Angeles (unpublished).

[4] W. F. Baker, R. L. Cool, E. W. Jenkins, T. F. Kycia, S. J. Lindenbaum, W. A. Love, D. Lüers, J. A. Niederer, S. Ozaki, A. L. Read, J. J. Russel, and L. C. L. Yuan, Phys. Rev. Letters **7**, 101 (1961).

[5] V. L. Fitch, S. L. Meyer, and P. A. Piroué, Phys. Rev. **126**, 1849 (1962).

[6] A. Schwarzschild and Č. Zupančič, Phys. Rev. **129**, 854 (1963).

[7] V. T. Cocconi, T. Fazzini, G. Fidecaro, M. Legros, N. H. Lipman, and A. W. Merrison, Phys. Rev. Letters **5**, 19 (1960).

[8] L. Gilly, B. Leontic, A. Lundby, R. Meunier, J. P. Stroot, and M. Szeptycka, in *Proceedings of the 1960 Annual International Conference on High-Energy Physics at Rochester* (Interscience Publishers, Inc., New York, 1960), p. 808.

[9] G. Von Dardel, R. M. Mermod, G. Weber, and K. Winter, in *Proceedings of the 1960 Annual International Conference on High-Energy Physics at Rochester* (Interscience Publishers, Inc., New York, 1960), p. 837

[10] D. Dekkers, J. A. Geibel, R. Mermod, G. Weber, T. R. Willits, K. Winter, B. Jordan, M. Vivargent, N. M. King, and E. J. N. Wilson, Phys. Rev. **137**, B962 (1965).

[11] R. A. Lundy, T. B. Novey, D. D. Yovanovitch, and V. L. Telegdi, Phys. Rev. Letters **14**, 504 (1965).

[12] A. C. Melissinos, T. Yamanouchi, G. G. Fazio, S. J. Lindenbaum, and L. C. L. Yuan, Phys. Rev. **128**, 2373 (1962).

[13] D. E. Dorfan, J. Eades, L. M. Lederman, W. Lee, C. C. Ting, P. Piroué, S. Smith, J. L. Brown, J. A. Kadyk, and G. H. Trilling, Phys. Rev. Letters **14**, 995 (1965).

[14] S. T. Butler and C. A. Pearson, Phys. Rev. Letters **7**, 69 (1961); **1**, 77 (1962); Phys. Rev. **129**, 836 (1963).

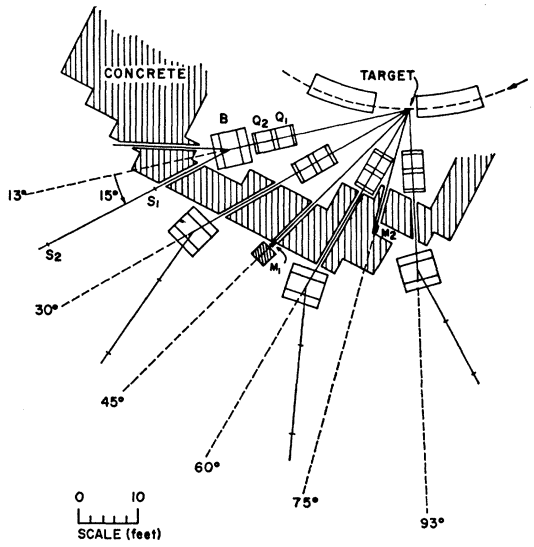

FIG. 1. Layout of the beams.

Q_1-Q_2, a bending magnet B, and two scintillation counters, S_1 and S_2. At 13°, where the stray field from the machine could not be neglected, a 30 in. long, 2 in. wide, 4 in. high magnetic shield (not shown in the figure) was placed near the synchrotron magnet.

Particles in a beam were identified by mass analysis. The momentum was selected by magnetic deflection and the velocity determined by time-of-flight measurements made between the two counters S_1 and S_2. Depending on the momentum the distance S_1-S_2 varied from 10 to 20 ft. The sizes of the counters were changed frequently in order to optimize the counting rate and minimize the losses due to multiple scattering (in S_1 primarily). Typically S_1 was $\frac{1}{8}$ in. thick, S_2 $\frac{1}{4}$ in. thick. The width and height ranged from $\frac{1}{4}$ in.$\times\frac{1}{4}$ in. to 2 in. $\times$2 in. for S_1, and 2 in.$\times$2 in. to 6 in.$\times$6 in. for S_2. The scintillation material was Pilot B. All counters were connected to Amperex 56AVP photomultipliers with Lucite light pipes shaped in such a way as to present to the incoming light a cross section of rigorously constant area. These light pipes, which have been described elsewhere,[15] are particularly well suited for timing purposes because of their high efficiency for light collection.

B. Electronics System

The electronics system, as shown in Fig. 2, was very simple. A wide resolution coincidence (C) is made between S_1 and S_2, using the anode pulses properly shaped by fast discriminators (A_1 and A_2). The coincidence $C=A_1A_2$ which indicates that a particle went through S_1 and S_2 must be wide enough so that the entire mass range one is interested in can be investigated concurrently. The dynode pulses, shaped by fast discriminators (D_1 and D_2) and gated by the coincidence C in the circuits C_1 and C_2, serve as timing pulses. The time difference between D_1 and D_2 is converted into pulse height and analyzed in a 512-channel pulse-height analyzer.

One of the limiting factors in mass spectroscopy by time-of-flight technique is the shifts in time produced by variations of pulse amplitude. These shifts result in a broadening of the peaks in the time-of-flight distributions. This effect, particularly serious for those pulses which are close to the discrimination level, is easily avoided here by setting the threshold of the D discriminators at a lower level than that of the A discriminators. The time resolution of the apparatus is also very much dependent on the size and thickness of the scintillators. Figure 3 shows a time-of-flight spectrum taken with $\frac{1}{2}$-in.$\times\frac{1}{2}$-in.$\times\frac{1}{8}$-in. and 2-in. $\times$2-in.$\times\frac{1}{4}$-in. counters as S_1 and S_2, respectively. The time resolution, as measured by the full width of the π peak at half maximum, is 0.7 nsec. A better resolution was achieved with thicker counters.

Another technique was used to detect K mesons which, especially at large distances, constitute a very small fraction of the counting rate ($\sim$0.01% to 0.001%). This technique, which has been described in detail elsewhere,[16] takes advantage of the rf structure of the PPA internal proton beam. The strong coupling between the radio frequency (rf) voltage and the proton beam at the end of the acceleration cycle causes the circulating protons to strike the target in 1.4-nsec wide bunches with a frequency of $\sim$30 Mc/sec, the frequency of the rf at full energy. Obviously this structure is still present in secondary beams and the precise timing provided by the rf can be used for time-of-flight measurements from the target to the detector. For example,

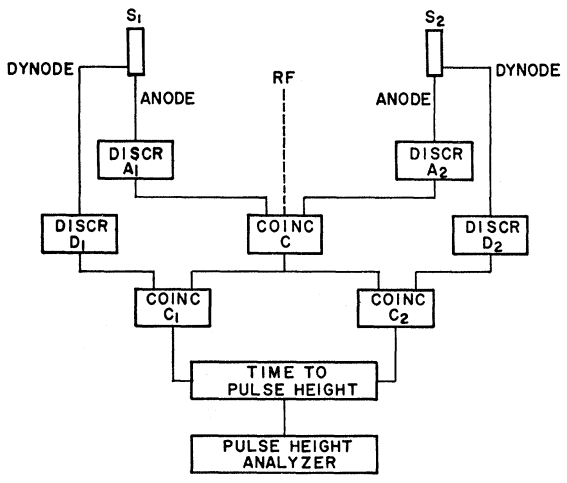

FIG. 2. Block diagram of the electronic system.

[15] P. A. Piroué, Natl. Acad. Sci.—Natl. Res. Council, Publ. 1184 (1964); Nucl. Sci. Ser. 40, 46 (1964).

[16] P. A. Piroué and A. J. S. Smith, IEEE Trans. Nucl. Sci. NS-12, 249 (1965), and PPAD-2137-545, Princeton-Pennsylvania Accelerator, Princeton University, Princeton, New Jersey, 1965 (unpublished).

one can limit the mass range investigated to the K-mass region simply by requiring a coincidence $C=A_1A_2$(rf) with the phase of the rf signal properly adjusted. This, in general, will result in an enormous reduction of background, as is seen in the time-of-flight spectrum shown in Fig. 4. The K^+-meson intensity at the last counter was 3 per 10^5 positive particles.

C. Beam Monitor

The internal proton beam striking the target was monitored by two three-counter telescopes, M_1 and M_2, located at 45° and 75°, respectively, and directed at the target (Fig. 1). The counter sizes were such that the ratio of their counting rates, M_1/M_2, was of the order of 100. Thus any deviation from linearity between the monitor and the beam on target because of dead time or pile-up problems, or simply malfunctioning, was readily detected.

Much attention was given to calibrating the monitor against the circulating protons. The voltage induced by the internal proton beam on an electrostatic probe was sampled before the beam struck the target, photographed on a fast oscilloscope, and compared to the monitor reading. This operation was repeated hundreds of times during the beam survey period and the results were found to be internally consistent.

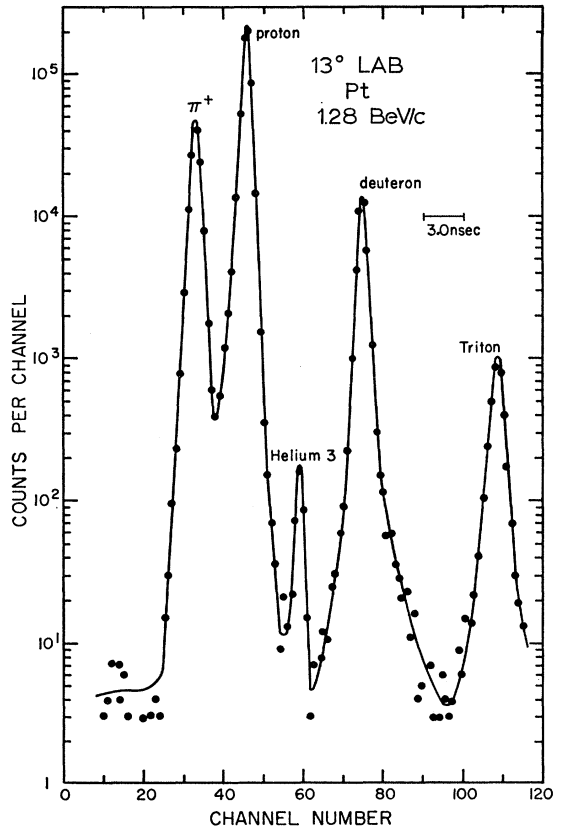

FIG. 3. Time-of-flight spectrum for 1.28 BeV/c positive particles emitted at 13° lab from a Pt target. The counter separation was 16 ft. The He^3 momentum is 2.56 BeV/c because of its double charge.

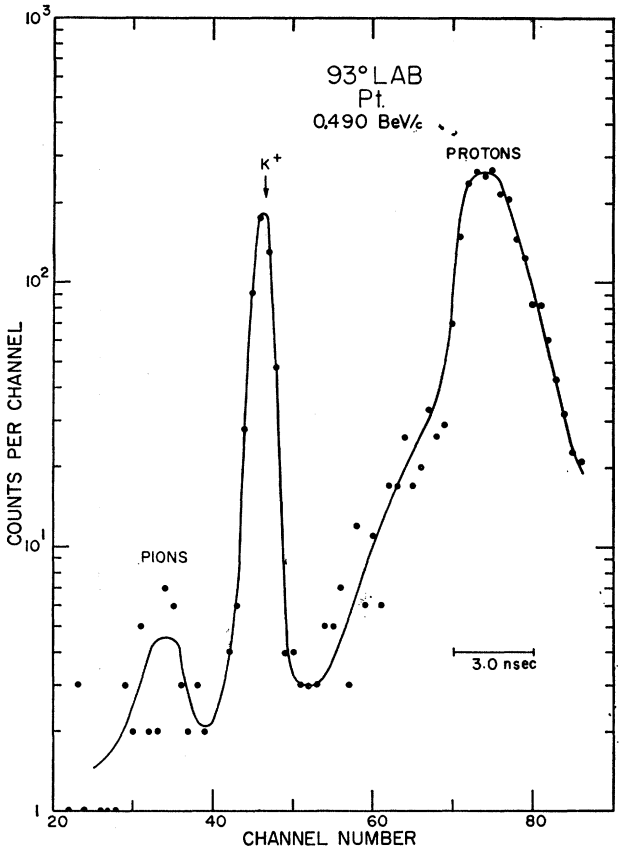

FIG. 4. Time-of-flight spectrum for 0.490 BeV/c positive particles emitted at 93° lab from a Pt target. Because of the rf coincidence requirement only K mesons were detected with full efficiency.

While the relative accuracy of the monitor is good to ~1%, the absolute calibration is known only to within 20% because of the inherent difficulties in measuring the circulating beam intensity.

III. RESULTS

A. General

The data taken at each magnet setting (i.e., each momentum) consisted of time-of-flight spectra similar to the one shown in Fig. 3. Relative yields of the various particles were obtained by integration of the corresponding peaks in the spectra. In order to obtain absolute cross sections, one must know the solid angle subtended by the detector, and the momentum resolution. A computer program, OPTIK,[17] was used to determine these quantities for each counter geometry. The data were, in general, taken with the quadrupoles turned off except when a well-defined beam and a large solid angle were needed (e.g., K-meson runs). Since the presence of quadrupoles modifies the solid angle and

[17] T. J. Devlin, Lawrence Radiation Laboratory Report No. UCRL-9727, 1961 (unpublished).

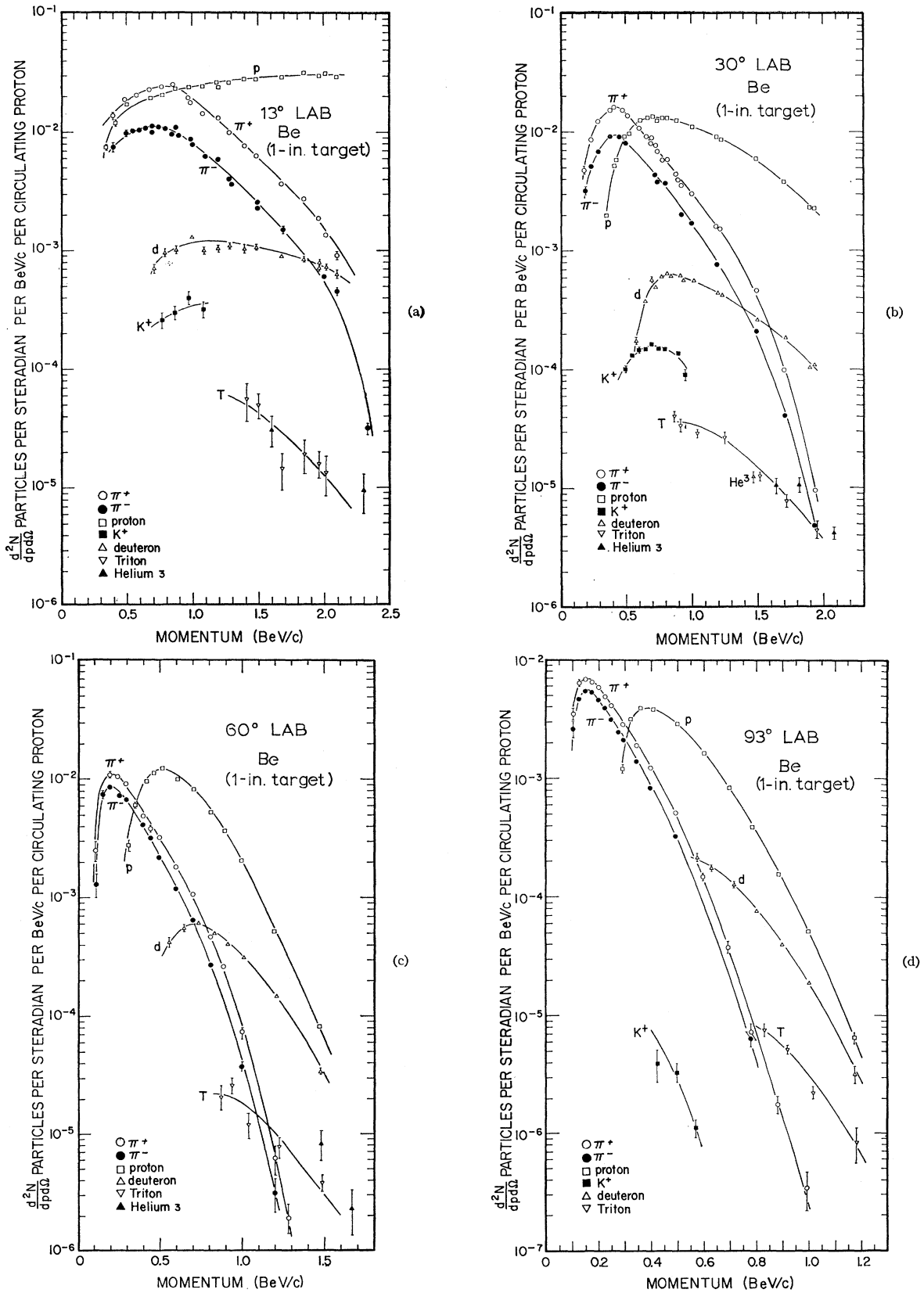

FIG. 5. Momentum spectra of particles emitted at (a) 13°, (b) 30°, (c) 60°, and (d) 93° in the laboratory from a beryllium target struck by 2.9-BeV protons. The ordinate is the number of particles produced in a 1-in. target per steradian per BeV/c per circulating proton; one particle corresponds to a cross section of 3.2×10^{-24} cm^2/sr (BeV/c) nucleus. The indicated errors include the statistical errors as well as the uncertainty introduced through corrections and other systematic sources (excluding absolute calibration which is known to within 20%). At 60° K mesons were not measured. No He^3 was observed at 93°.

TABLE I. Differential cross sections in the laboratory system for antiproton production from Be and Cu at 13° and 760 MeV/c. The data are those of Ref. 13.

Target	Incident proton kinetic energy (BeV/c)	Number of $\bar{p}$ events	$\bar{p}/\pi^-$ ratio (10^{-10})	$\frac{d^2\sigma}{dpd\Omega}\left(\frac{10^{-35}\text{ cm}^2}{\text{(BeV/}c\text{) sr nucleon}}\right)$
Be	2.88	0	<3.0	<4.0
Cu	2.88	4	6.3±3.2	8.2±4.0
Cu	3.05	5	9.2±3.8	11.5±4.6

the momentum resolution, yet leaves the relative yields unaltered, a point measured with the quadrupoles on was always compared to the data obtained with the quadrupoles off so that this point could be properly normalized.

Corrections were made for (a) multiple Coulomb scattering, (b) nuclear absorption, and, when appropriate, (c) particle decay, and (d) electron and μ-meson contamination. These corrections are described below.

The experimental results for various laboratory angles are shown in Fig. 5 (Be) and Fig. 6 (Pt). In both figures the yield $d^2N/dpd\Omega$ [expressed as the number of particles produced in a 1-in. target per steradian (BeV/c) (circulating proton)] is displayed as a function of laboratory momentum. In all cases the energy of the incoming protons was 2.9±0.1 BeV. The indicated errors include the statistical errors as well as the uncertainty introduced through the application of the above corrections, but they do not include the 20% uncertainty in absolute calibration described in Sec. IIC.

Both the Be and Pt targets were 1 in. long, $\frac{1}{2}$ in. wide, and $\frac{1}{4}$ in. high. In addition a 0.060-in.-thick Be lip (thin foil) was placed on the outside of the target. The energy loss in the lip caused the beam to shift slightly inward, and thus to traverse the target in its entire length. But, because of the energy loss in the target itself, the beam could not recirculate around the synchrotron and strike the target again. Therefore, the yields can be readily converted into differential cross sections. The following factors convert the yields $d^2N/dpd\Omega$ into differential cross sections expressed in cm²/[sr (BeV/c) nucleus]: 3.2×10^{-24} for beryllium, 6.4×10^{-24} for platinum.[18]

With regard to K mesons it was not always possible to obtain a momentum spectrum because of the extra difficulties involved and the limited time available. At 60°, for example, we had no time even to look for K mesons.

Finally, for the sake of completeness, we present in Table I the results, already reported,[13] on antiproton production in various target materials at 13° and 760 MeV/c laboratory momentum. As mentioned above these results were obtained in a separate experiment performed in collaboration with a Columbia University group.

B. Corrections

(a) Because of the difficulty of calculating losses caused by multiple scattering in the front counter and in the air, the counter geometry was always such that these losses were minimized (<10% in most cases). We relied on calculations similar to those of Sternheimer,[19] but adapted to a rectangular geometry, to evaluate the corrections. We checked them at various momenta by changing the counter geometry and found them to be reliable to within 25%.

(b) Nuclear absorption in the air and in the front counter never amounted to more than 12%.

(c) Corrections were applied for the decay of π and K mesons along the beam.

(d) Up to 400 MeV/c the electron and μ-meson contaminations of the beams could be measured directly by time-of-flight technique. As expected they were strongly dependent on the beam geometry. Furthermore the electron contamination which, at very low momenta, could be as high as 90%, depended also very much on the angle of production and the target material. Above 400 MeV/c, both the muon and electron contaminations were calculated by using expressions which agreed reasonably well with the measurements made at lower momenta. At all angles but 13° the over-all correction at 400 MeV/c did not exceed 20%. At 13° it was so much higher (~50%) that we had to use measurements made by others[1] with a Čerenkov counter to determine the corrections at higher momenta.

IV. INTERPRETATION OF THE RESULTS

A. Introduction

Although the detailed mechanisms for particle production in high-energy proton-nucleus collisions are not

[18] Corrections due to the finite length of the targets are included (~8% for Pt and negligible for Be).

[19] R. M. Sternheimer, Rev. Sci. Instr. 25, 1070 (1954).

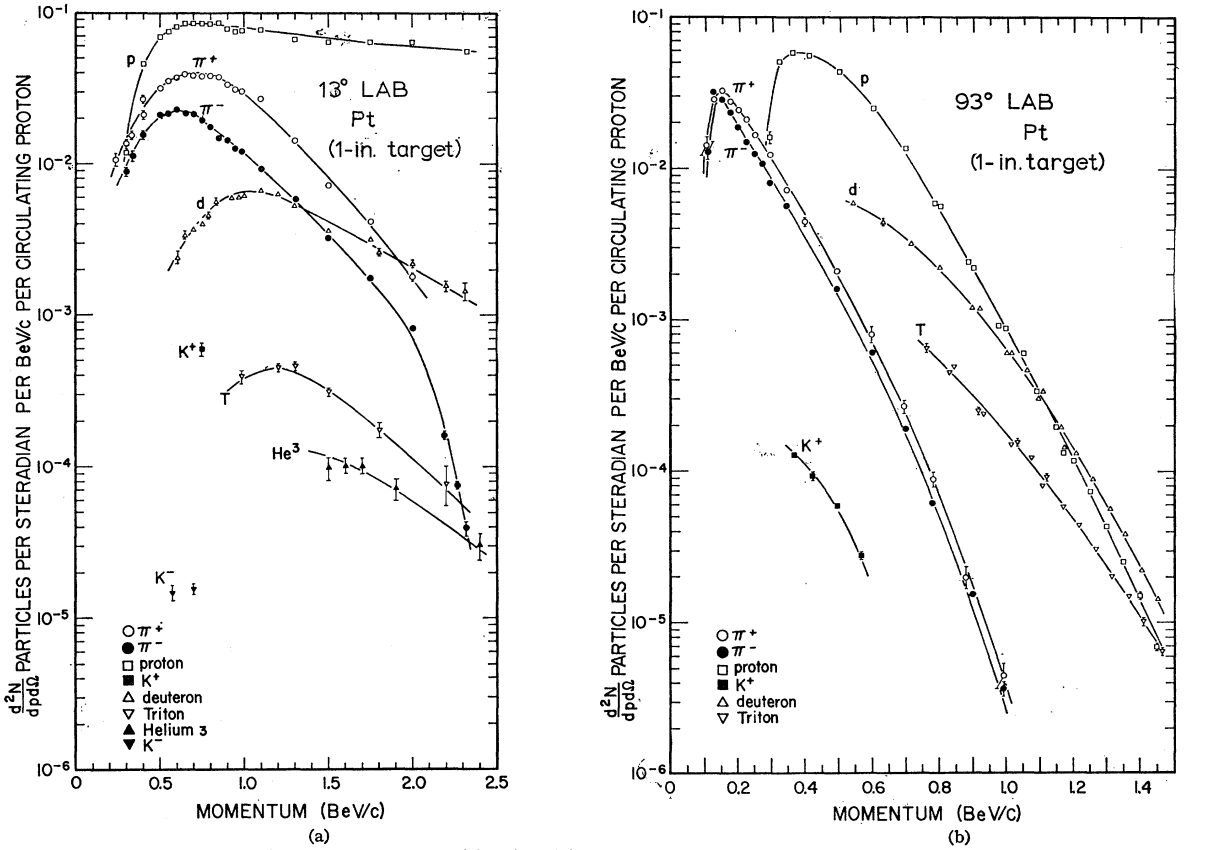

FIG. 6. Momentum spectra of particles emitted at (a) 13° and (b) 93° in the laboratory from a 1-in. platinum target struck by 2.9-BeV protons. One particle corresponds to a cross section of 6.4×10^{-24} cm²/sr (BeV/c) nucleus. No He^3 was observed at 93°. For general remarks refer to Fig. 5 caption.

known, it can be expected that for incident momenta $\gg\hbar/R$ (R is the nucleon radius), the incoming proton interacts with individual target nucleons rather than with the nucleus as a whole. Indeed evidence of this has been observed in many reactions.[20] However, because of Fermi motion (motion of nucleons bound in the nucleus) proton-nucleus collisions can have different distributions of final states than do collisions in which the target nucleon is at rest. For example, reaction channels forbidden in p-p collisions may be opened in proton-nucleus collisions because of extra energy available in the c.m. system. Another consequence of Fermi motion is the broadening of the momentum distributions of reaction products, broadening particularly noticeable in reactions resulting in two-body final states. In many-body final states, broadening should also occur, but to a lesser extent. This point is further discussed below in the analysis of the pion and proton spectra.

It is interesting to note that the nucleus can also interact as a whole even when the momentum of the incoming particle is $\gg\hbar/R$. Coherent processes, i.e., processes in which the amplitudes of the individual target nucleons add with a definite phase, have been observed in π-nucleus interactions at multi-BeV energies.[21–24] In particular, final states consisting of a multipion system and an intact recoil nucleus exhibit, in some cases, an angular distribution characteristic of the radius of the target nucleus. Evidence for coherent photoproduction reactions with complex nuclei has also been reported.[25]

In the analysis below we first compare, for each particle, the experimental momentum spectra (Figs. 5–6) to the corresponding data in hydrogen. Models which have been successful in interpreting the general features of particle production in p-p collisions at 3 BeV are modified to take into account Fermi motion, and then are compared with the experimental results. In some cases the agreement is excellent (e.g., π

[20] For a review see S. J. Lindenbaum, Ann. Rev. Nucl. Sci. **7**, 317 (1957).

[21] J. F. Allard, D. Drijard, J. Hennessy, R. Huson, A. Lloret, J. Six, J. J. Veillet, G. Bellini, M. di Corato, E. Fiorini, P. Negri, M. Rollier, J. Crussard, J. Ginestet, A. H. Tran, H. H. Bingham, R. Diebold, W. B. Fretter, H. J. Lubatti, W. Michael, and K. Moriyasu, Phys. Letters **19**, 431 (1965).

[22] J. D. Rinaldo, P. L. Jain, and P. D. Bharadwaj, Nuovo Cimento **36**, 1089 (1965); and A. Caferio *et al.*, *ibid.* **32**, 1471 (1964).

[23] M. A. Abolins, D. D. Carmony, R. L. Lander, and Hg. H. Xuong, Phys. Rev. Letters **15**, 125 (1965); and I. Butterworth, J. L. Brown, G. Goldhaber, S. Goldhaber, A. A. Hirata, J. A. Kadyk, and G. H. Trilling, *ibid.* **15**, 500 (1965).

[24] G. Vegni, H. Winzeler, P. Zaniol, P. Fleury, and G. de Rosny, Phys. Letters **19**, 526 (1965).

[25] L. J. Lanzerotti, R. B. Blumenthal, D. C. Ehn, W. L. Faissler, P. M. Joseph, F. M. Pipkin, J. K. Randolph, J. J. Russel, D. G. Stairs, and J. Tenenbaum, Phys. Rev. Letters **15**, 210 (1965).

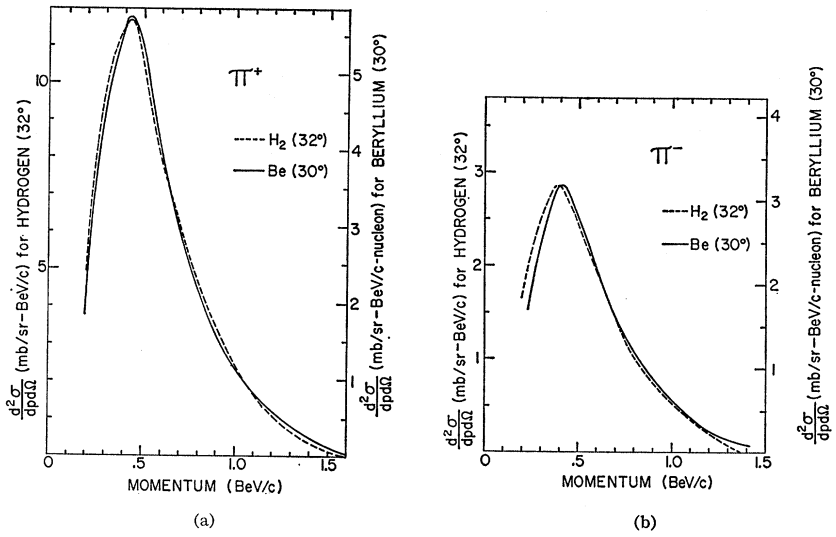

FIG. 7. Comparison between the π-momentum distributions obtained at 30° from Be (solid line), and at 32° from H_2 (dashed line). The H_2 data are those of Melissinos *et al.* (Ref. 12).

mesons). In other cases the method fails completely (e.g., deuterons), suggesting that different processes, characteristic of the nucleus, take place.

B. π Mesons

1. Comparison of p-Nucleus and p-p Results

Differential cross sections for the production of $\pi^{\pm}$ mesons in 2.9-BeV p-p collisions have been measured at laboratory angles of 0°, 17°, and 32° by Melissinos *et al.*[12] Their 32° results are compared with our 30° Be data in Fig. 7. In each case the momentum distributions are normalized to equal areas. It is quite evident that there is no significant difference between the shapes of the two curves for either positive or negative pions. This indicates that (a) π-meson production in p-Be collisions results from nucleon-nucleon encounters, (b) the momentum spectra of π^+ and π^- mesons produced in p-p and p-n collisions are essentially the same, and (c) the effect of Fermi motion is negligible. Similar conclusions have already been reached at 1.0 and 2.3 BeV.[26]

Production of π mesons in carbon has also been measured at 32° by Melissinos *et al.*[12] Their results and ours are summarized in Table II. As expected the π^+-meson yield per nucleon is largest in hydrogen and there does not seem to be any significant difference between the Be and C data (in both experiments the absolute cross sections are known to within 15–20%) except possibly for the π^+/π^- ratio. In Pt however, the π-meson yield per nucleon is smaller by a factor 7–8 at 13°, and only $\sim$2.5 at 93°. Since one would expect 7.85 if only nuclear shielding effects were present $[(A_{Pt}/A_{Be})^{2/3}=7.85]$, this clearly indicates that re-absorption effects (i.e., primarily scattering) within the nucleus are negligible at 13°, but quite substantial at 93°, especially in a heavy nucleus such as Pt.

2. Models of π-Meson Production

Practically all experimental data on p-p collisions at $\sim$3 BeV lead to the conclusion that the $\frac{3}{2}$, $\frac{3}{2}$ isobar (N_{33}^*) of mass 1238 MeV plays a major role in inelastic processes.[12,27–30] Among the many theoretical models which have been proposed (e.g., isobar,[31] one-pion exchange,[32] extended isobar[33]), the isobar model predicts quite well the single-pion production which, at this energy, accounts for about half of the total pion pro-

TABLE II. Differential cross sections in the laboratory system for π-meson production from Be, Pt, C, and H_2 at various angles.

Target	Laboratory angle (deg)	$d\sigma/d\Omega$ (mb/sr-nucleon) π^+	π^-	π^+/π^- ratio
Be	13	8.40	3.58	2.35
	30	3.10	1.77	1.75
	60	1.22	0.895	1.36
	93	0.488	0.384	1.27
Pt	13	1.17	0.581	2.01
	93	1.94	0.151	1.29
C[a]	32	3.67	1.86	2.0
H_2[a]	32	6.48	1.64	4.0

[a] Data of Ref. 12.

[26] L. C. L. Yuan and S. J. Lindenbaum, Phys. Rev. **103**, 404 (1956).

[27] G. Smith, H. Courant, E. Fowler, H. Kraybill, J. Sandweiss, and H. Taft, Phys. Rev. **123**, 2160 (1961).

[28] E. Hart, R. Louttit, D. Lüers, T. Morris, W. Willis, and S. Yamamoto, Phys. Rev. **126**, 747 (1962).

[29] G. Chadwick, G. Collins, C. Schwartz, A. Roberts, S. DeBenedetti, N. Hien, and P. Duke, Phys. Rev. Letters **4**, 611 (1960).

[30] G. Chadwick, G. Collins, P. J. Duke, T. Fujii, N. Hien, A. Kemp, and F. Turkot, Phys. Rev. **128**, 1823 (1962).

[31] S. J. Lindenbaum and R. M. Sternheimer, Phys. Rev. **105**, 1874 (1957).

[32] F. Selleri, Phys. Rev. Letters **6**, 64 (1961).

[33] R. M. Sternheimer and S. J. Lindenbaum, Phys. Rev. **123**, 333 (1961).

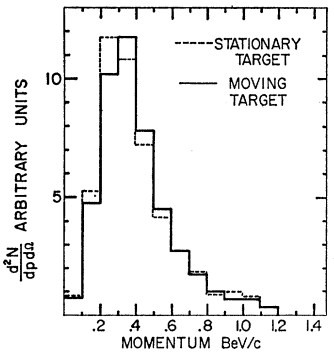

FIG. 8. Isobar model predictions for single-pion momentum distributions at 30° in the laboratory. The dashed line refers to a stationary target nucleon; the solid line to a target nucleon with a Gaussian momentum distribution corresponding to an average energy of 19.3 MeV.

duction. This model assumes that the N_{33}^* isobar is produced with an angular distribution strongly peaked forward-backward ($\cos^{16}\theta$) and that it subsequently decays isotropically in its own rest frame.

A model, to be consistent with our results, must account for the negligible effect of Fermi motion. We have tested this feature for the isobar model outlined above. Using a Monte Carlo method, we calculated the single-pion momentum distribution at 30° in the laboratory, first for a stationary target nucleon, and then for a target nucleon with a Gaussian momentum distribution, viz.,

$$f(p)d^3p = (3.64)^3 \exp(-41.2p^2)d^3p, \qquad (1)$$

where p is expressed in BeV/c. (This momentum distribution, used widely in the literature,[34] corresponds to an average kinetic energy of 19.3 MeV.) The results are shown in Fig. 8. It is clear that the inclusion of Fermi motion has no significant influence upon the isobar model predictions, in agreement with experiment. (Incidentally, Fermi motion does broaden considerably the single-pion momentum distribution given by phase space.) We have not considered multi-pion production because the effects of Fermi motion ought to be considerably reduced.

3. *Transverse Momentum Distributions*

It has been known for some time that, for bombarding energies $E \geq 20$ BeV, the transverse momentum distribution of π mesons is nearly independent of E and of the laboratory angle θ, and exhibits an exponential high-momentum tail.[35] The average transverse momentum of the pions is ~400 MeV/c. At 3 BeV, we do not expect these properties to hold true, because energy conservation limits the transverse momentum to lower values, especially at small angles θ with respect to the incident proton beam. We see in Fig. 9 however, plotting the yields $d^2N/dpd\Omega$ now as a function of the transverse momentum $p\sin\theta$, that the shapes of the resulting distributions as well as the average transverse momenta do not depend much upon θ. Such general behavior is predicted by the isobar model described above. These curves can be used to estimate the pion yields at other angles simply by interpolation.

C. K^+ Mesons

Many of the conclusions reached in the case of π-meson production seem to be equally valid for K^+-meson production, viz., (a) nucleon-nucleon encounters are responsible for production of K^+ mesons in proton-nucleus collisions, (b) the momentum spectra of K^+ mesons produced in p-p and p-n collisions are probably very similar, (c) Fermi motion does not play an important role, and (d) scattering within the nucleus constitutes—at least for heavy targets—the main source of K^+ mesons at large angles.

Just as in the case of the pions the evidence for (a), (b), and (c) comes from comparison of the 30° Be data with corresponding data in hydrogen. In a recent experiment at the PPA,[36] differential cross sections as a function of momentum were measured for the production of K^+ mesons at laboratory angles of 20°, 30°, and 40° in 2.9-BeV p-p collisions. At 30°, where a direct comparison can be made, we find no significant difference between the Be and H_2 data, except in the absolute value of the cross sections (the K^+ yield per nucleon is larger in H_2 by a factor ~1.4). The evidence for (d) comes from the comparison of the Be and Pt data at 13° and 93°. Although the data in some cases are scanty, there is no doubt that the effect observed for pions (i.e., the increased π yield in Pt relative to Be at large angles) is even more pronounced for K^+ mesons. At 93°, a Pt target produces ~20 times as many K^+ mesons as does a Be target of equal length while, at 13°, the ratio is only ~2.5. As a result experiments with low energy K^+ or K_2^0 mesons are best performed at large angles with heavy targets.

It has been pointed out in a previous communication[37] that the observed momentum distribution at 30° represents a violation of phase space. This fact has been confirmed in the p-p experiment mentioned in Ref. 36 and will be more fully discussed in a forthcoming paper on this subject.

D. Protons

Proton-proton scattering has been investigated at an incident kinetic energy of 2.9 BeV and laboratory angles ranging from 2° to 17° by Fujii *et al.*[38] (elastic) and Chadwick *et al.*[30] (inelastic). Their results at 12°

[34] See for example M. M. Block, E. M. Harth, and R. M. Sternheimer, Phys. Rev. **100**, 324 (1955).

[35] See, for example, G. Cocconi, L. J. Koester, and D. H. Perkins, University of California Radiation Laboratory Report No. UCRL SS-28-2, (or UCID-1444), 1961 (unpublished).

[36] W. Hogan, P. A. Piroué, and A. J. S. Smith (to be published).

[37] P. A. Piroué, Phys. Letters **11**, 164 (1964). Due to an error in the beam calibration the absolute value of the K^+-meson cross sections reported in this paper are overestimated by a factor ~6. This has, however, no bearing on the conclusions of the paper.

[38] T. Fujii, G. B. Chadwick, G. B. Collins, P. J. Duke, N. C. Hien, M. A. R. Kemp, and F. Turkot, Phys. Rev. **128**, 1836 (1962).

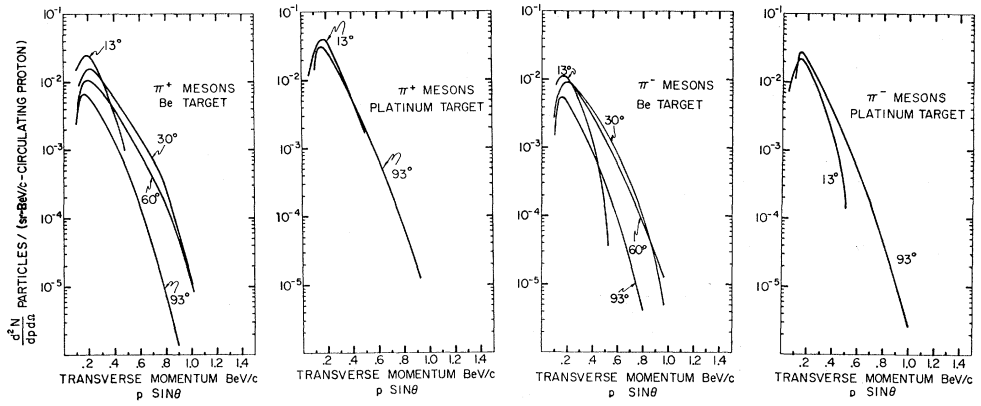

FIG. 9. Yields of π^+ and π^- mesons versus transverse momentum $p \sin\theta$.

can be directly compared to ours at 13°. Although our measurements do not extend to high enough momenta to observe the elastic peak and the peaks corresponding to the various isobars, we find that the inelastic protons from Be follow a similarly shaped distribution to those from H_2 (i.e., having a broad maximum at $\sim$2.2 BeV/c); those from Pt, however, reach a maximum at $\sim$700 MeV/c, indicating that some nuclear effect is present. Butler and Pearson[14] have suggested that a nucleon shower is generated when a high-energy proton collides with a nucleus. Indeed at 33 BeV Schwarzschild and Zupančič[6] have found that, on the average, about three nucleons are emitted per interacting proton. At 3 BeV, not enough data are available (especially at small angles) to perform such a calculation. Nevertheless it seems that a similar mechanism could well be responsible for the greatly enhanced production of low-energy protons in platinum. The analysis of the deuteron spectra further supports this assumption.

At 30° (and 13°) our measurements do not extend to high enough momenta to cover the elastic peak region. But at 60° they do and no peak whatsoever is observed ($\sim$860 MeV/c) within the resolution of our measurements. This fact was further investigated in the course of the experiment on K^+-meson production in p-p collisions mentioned in Ref. 36. The momentum spectra of protons emitted at 60° in the laboratory from Be and H_2 targets were measured. The results are shown in Fig. 10. The striking feature is the complete disappearance of the elastic peak in the proton spectrum from Be. In an attempt to explain this result we calculated the effect of Fermi motion upon the elastic peak of Fig. 9. Using the distribution (1) folded into the elastic part of the spectrum, we found that the peak is broadened by a factor $\sim$10 (and thus reduced in amplitude by the same factor). When the inelastic protons are included one realizes that Fermi motion accounts for the disappearance of the elastic peak in the proton spectrum from Be. At smaller angles, where the elastic cross sections are larger, it is possible that some enhancement remains, as Cocconi *et al.*[39] have observed at higher energies.

Finally, at 93° the proton yield in Pt relative to Be is found to be much larger than at 13°. This effect has already been discussed in connection with the pion and K^+-meson spectra.

E. Deuterons

Deuteron production at laboratory angles larger than 23° is forbidden in 2.9-BeV p-p collisions. This kinematical limit increases to 32° when the target nucleon is allowed a Fermi energy of 20 MeV. Therefore, the copious production of deuterons observed at 30°, 60°, and 93° from Be and Pt targets can be taken as clear evidence that nuclear matter plays a major role in deuteron production in complex nuclei. This fact is further confirmed by the comparison of the total cross section for deuteron production in p-Be collisions ($\sim$1 mb per nucleon at 2.9 BeV) with the cross section for the reaction $p+p \rightarrow d+\pi^+$ (30$\pm$3 μb at the same energy).[40] Even when multi-pion final states are included, the total cross section for deuteron production in H_2

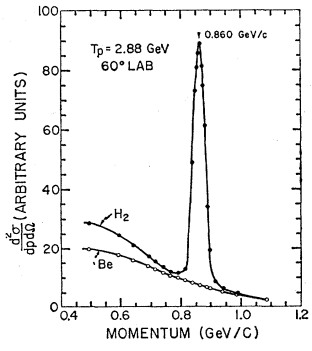

FIG. 10. Momentum spectra of protons emitted at 60° lab from hydrogen and beryllium targets struck by 2.88-BeV protons.

[39] G. Cocconi, A. N. Diddens, E. Lillethun, and A. M. Wetherell, Phys. Rev. Letters **6**, 231 (1961).

[40] O. E. Overseth, R. M. Heinz, L. W. Jones, M. J. Longo, D. E. Pellett, M. L. Perl, and F. Martin, Phys. Rev. Letters **13**, 59 (1964).

should not amount to more than 10% of the cross section (per nucleon) in Be.

Deuteron production in complex nuclei has also been measured at higher bombarding energies[5–7] (10–30 BeV), and the analysis of the results leads to a similar conclusion, viz., nuclear matter plays a dominant role. As already mentioned in connection with the proton spectra, Butler and Pearson[14] have suggested that a shower of nucleons develops within a nucleus struck by a high-energy proton. These authors have proposed a mechanism for deuteron formation which involves the pairing of a neutron and proton of roughly equal momenta from the shower nucleons. Models[6,14] based on these assumptions interpret reasonably well some of the features of the experimental observations at high energies. The characteristics of all these models is that they provide a connection between the number of deuterons emerging at a given angle and momentum, and the corresponding number of protons at that angle, but at *half* that momentum.

It is tempting to try to understand our deuteron data, especially the momentum dependence exhibited by the various spectra, along similar lines. As a first attempt let us assume that (i) at a given angle the shower distributions of *both* protons and neutrons are given by the experimentally observed proton distribution; (ii) deuterons are formed from pairs of neutrons and protons with approximately equal momenta; (iii) the probability of deuteron formation is proportional to the time T spent by the nucleons within the nucleus (the nuclear field is necessary to absorb recoil). Let $D(\mathbf{k})d^3k$ be the number of deuterons formed per collision with momentum between $\mathbf{k}$ and $\mathbf{k}+\mathbf{dk}$. According to the above assumptions, this number will be proportional to T, i.e., to $1/k$, and also to the square of the proton distribution P evaluated at momentum $\mathbf{k}/2$:

$$D(\mathbf{k})d^3k \propto P^2(\tfrac{1}{2}\mathbf{k})d^3k/k. \tag{2}$$

Since all our results are presented in terms of the number of particles produced in a 1-in. target, per steradian per BeV/c per circulating proton, we want to relate $D(\mathbf{k})$ and $P(\frac{1}{2}\mathbf{k})$ to these quantities, viz., $d^2N_d(\mathbf{k})/dkd\Omega$ and $d^2N_p(\frac{1}{2}\mathbf{k})/dkd\Omega$, respectively. If η is the fraction of the incident proton beam interacting in the 1-in. target ($\sim$0.08 in Be and $\sim$0.30 in Pt), we have

$$d^2N_d(\mathbf{k})/dkd\Omega=\eta k^2 D(\mathbf{k}), \tag{3}$$

and

$$d^2N_p(\tfrac{1}{2}\mathbf{k})/dkd\Omega=\eta(\tfrac{1}{2}k)^2P(\tfrac{1}{2}\mathbf{k}). \tag{4}$$

The over-all momentum dependence of the deuteron yield is then

$$d^2N_d(\mathbf{k})/dkd\Omega=C[d^2N_p(\tfrac{1}{2}\mathbf{k})/dkd\Omega]^2/\eta k^3, \tag{5}$$

where C is a constant of proportionality, hopefully independent of the angle of production.

To compare the expression (5) with the observed deuteron spectra at each angle we have chosen C to fit the deuteron yield predicted by (5) to the experimental yield at 1.2 BeV/c. The results are shown in Fig. 11 together with the values obtained for C. The agreement between the curves is in general quite good above $\sim$1 BeV/c. At lower momenta, however, the expression (5) predicts fewer deuterons than observed. With regard to C the agreement is not spectacular (there seems to be a definite angular dependence); but it is not completely discouraging in view of the simplicity of the model. It seems that similar difficulties are also encountered with this kind of approach at higher energies.[41] The close agreement at corresponding angles between the values in Be and in Pt suggests that C is independent of the nucleus.

A possible mechanism which could provide additional deuterons at low momenta is the pairing of shower nucleons and nucleons in the tail of the Fermi distribution. Using a momentum distribution of the form

$$f(p)d^3p=\frac{10.6}{1+e^{(p-0.10)/0.05}}d^3p, \tag{6}$$

where p is expressed in BeV/c, we obtained some improvement, but unfortunately not in all cases. This distribution, which corresponds to an average Fermi energy of 20 MeV, is discussed in the analysis of the antiproton data. It should be mentioned that the Gaussian distribution (1) does not have a long enough tail to give any substantial contribution by this process.

In any case it appears—just as is the case at higher energies—that some of the features of deuteron production in complex nuclei are reasonably well explained by this model. But, of course, many problems remain, which could perhaps be of interest to nuclear theorists.

F. Tritons and Helium-3

The observed production of tritons and He^3 is obviously of nuclear origin since these particles cannot be produced at all in 2.9-BeV p-p collisions. The great similarity between the shapes of the momentum distributions of deuterons, tritons, and He^3 further suggests that identical mechanisms are responsible for their production. Extending to tritons and He^3 the model used for deuterons, one obtains that the triton-to-deuteron ratio should be of the same order of magnitude as the deuteron-to-proton ratio at any given angle and any given momentum per nucleon, i.e.,

$$n_t(3\mathbf{k})/n_d(2\mathbf{k})\cong n_d(2\mathbf{k})/n_p(\mathbf{k}), \tag{7}$$

where $n(\mathbf{k})$ denotes the yields $d^2N/dkd\Omega$ at momentum

[41] In the model proposed by Butler and Pearson in Phys. Rev. 129, 836 (1963), the deuteron formation probability is proportional to $|V_0|^2$, where $|V_0|$ is the magnitude of the optical potential depth. It is claimed in this paper that comparison with the data yields, in all cases, a value of 25±5 MeV for $|V_0|$. Using the same data and the same formula [Eq. (34)] we do not obtain this result. We find that we cannot fit the data of Figs. 4, 5, and 6 of this paper without using widely differing values of $|V_0|$, viz., 110, 41, and 71 MeV, respectively.

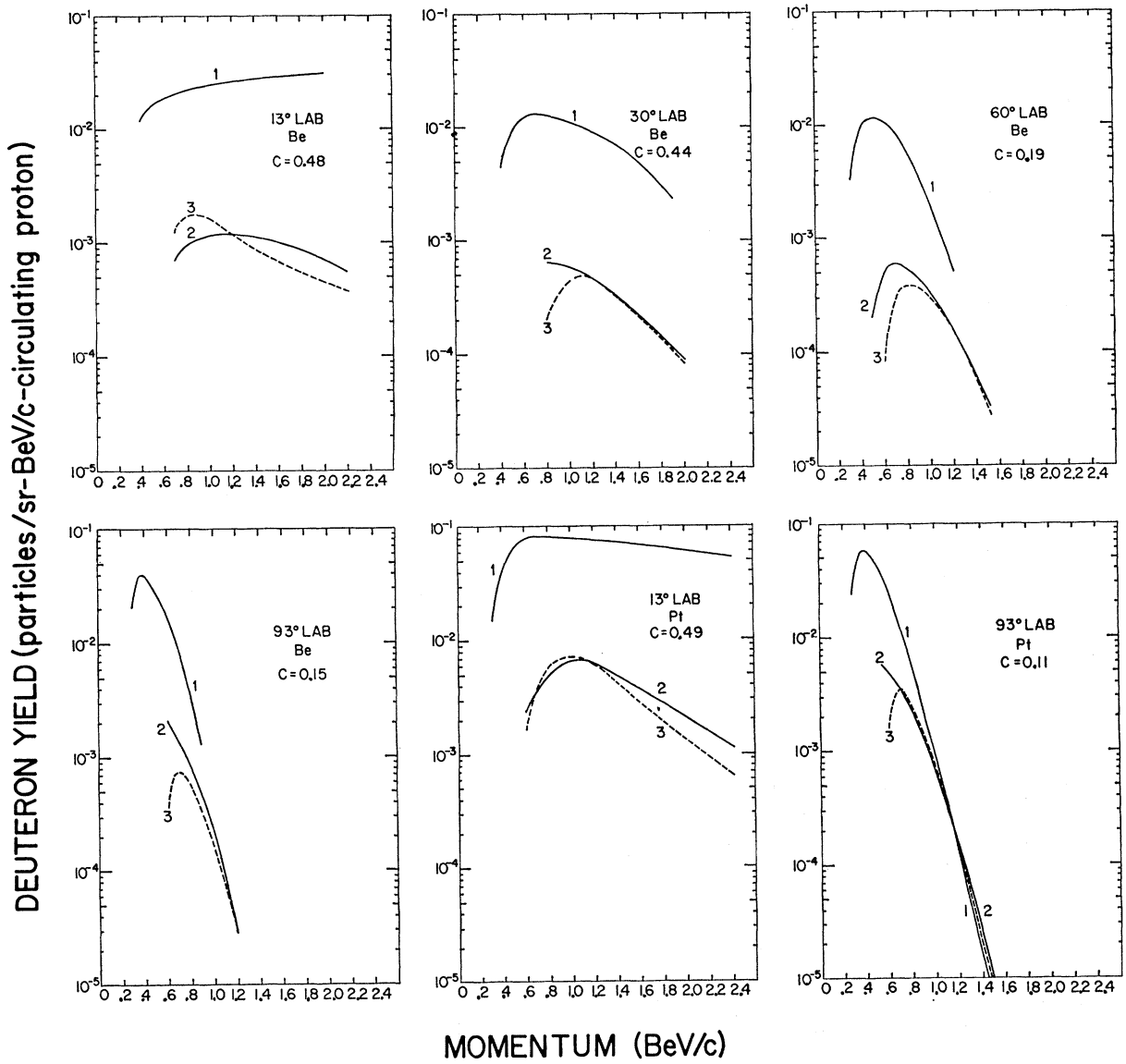

FIG. 11. Comparison between the experimental and calculated deuteron spectra for various targets and laboratory angles. Curves 2 and 3 are the observed and calculated deuteron spectra, respectively. Curves 1 are the experimental proton spectra. The values indicated for C are those which fit the deuteron yields predicted by (5) to the experimental yields at 1.2 BeV/c.

k. Within the limited range of our momentum measurements the experimental observations are in qualitative agreement with this relation. This has also been verified at higher energies.[6]

G. Antiprotons

The antiproton data presented in Table I and the data obtained at higher bombarding energies[13,42] (3.5–6.1 BeV) have been analyzed in a previous publication.[13] Therefore, no analysis will be given here, only results (old and new).

[42] Owen Chamberlain, Emilio Segrè, Clyde Wiegand, and Thomas Ypsilantis, Phys. Rev. **100**, 947 (1955).

The main objective of this work was the investigation of the tail of the momentum distribution of nucleons inside the nucleus. This was accomplished in a series of measurements on the reaction

$$p+\mathrm{Cu}\rightarrow\bar{p}+\text{residue} \tag{8}$$

with protons of energies near and below threshold for antiproton production via the free-particle reaction

$$p+\binom{n}{p}\rightarrow p+\binom{n}{p}+p+\bar{p}. \tag{9}$$

The results, expressed in the form of number of antiprotons produced relative to π^- mesons as a func-

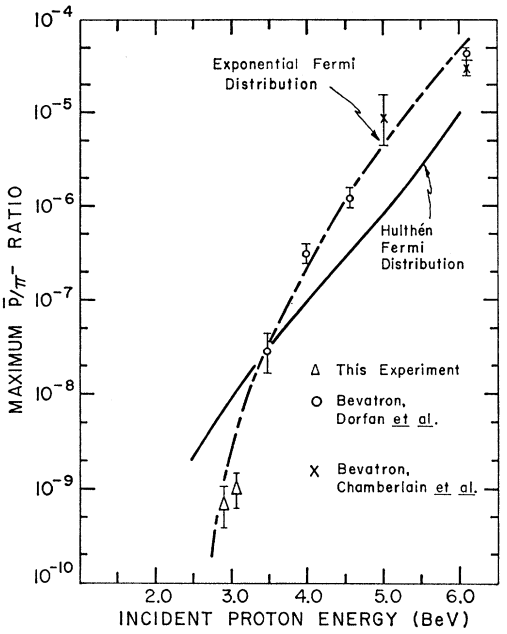

FIG. 12. Maximum $\bar{p}/\pi^-$ yields versus incident proton energy. The data are those of Ref. 13 and of Chamberlain *et al.* (see Ref. 42). The solid line represents the fit obtained with the momentum distribution (10), the dashed line with the distribution (11). In both cases Fermi motion in *all* directions has been considered (see Ref. 43). The normalization at the 3.5-BeV point is arbitrary.

tion of incident proton energy, were found to disagree completely with the hypothesis of a Gaussian distribution with mean energy of 20 MeV. Fair agreement between data and calculation was obtained with a momentum distribution of the Hulthén type, viz.,

$$f(p)d^3p \propto d^3p/(p^2+\alpha^2)(p^2+\beta^2), \qquad (10)$$

where $\alpha=0.047$ BeV/c, $\beta=7\alpha$, and $p_{\max}=1.0$ BeV/c (cutoff).

Recently, we have noticed that with a function of the form $\exp(-p/\lambda)$, where $\lambda=0.05$ BeV/c, one can fit quite well the data obtained at the lowest energies (corresponding to the highest Fermi momenta), even without applying any cutoff. At small momenta, however, this function is not acceptable since it is known from low-energy experiments that the Fermi distribution is approximately square in shape with a mean energy of $\sim$20 MeV. Therefore, we have tried the following distribution:

$$f(p)d^3p \propto \frac{d^3p}{1+e^{(p-p_0)/\lambda}}, \qquad (11)$$

which has the required behavior both at low and high momenta, and gives an average nucleon energy of 20 MeV when $p_0=0.10$ BeV/c. The excellent fit obtained with this distribution, as shown by the dashed curve of Fig. 12, strongly suggests that the tail of the Fermi momentum distribution is indeed exponential in shape.[43]

ACKNOWLEDGMENTS

The authors express their gratitude to Professor M. G. White and the members of the staff of the Princeton-Pennsylvania Accelerator for their invaluable cooperation throughout the course of this experiment. They are particularly indebted to Professor F. C. Shoemaker, Professor A. Lemonick, and J. Kirchgessner whose untiring efforts during this initial experimental period were essential to the progress of this work. Many thanks are also due M. V. Isaila for the considerable help he provided in the calibration of the internal proton beam. Finally we acknowledge the assistance of W. J. Hogan and L. S. Schulman in the taking of data, and of U. Gerlach and R. S. Remmel in the analysis of the results.

[43] The inclusion of Fermi motion in all directions has two effects: (a) It modifies the c.m. total energy available, and (b) it changes the direction of the c.m. velocity. In the Hulthén fit presented in Ref. 13, (b) has been neglected.